Signal Processing 96 (2014) 228–240

Contents lists available at ScienceDirect

Signal Processing

journal homepage: www.elsevier.com/locate/sigpro

Review

# A Bayesian approach for adaptive multiantenna sensing in cognitive radio networks ☆

J. Manco-Vásquez [a,*], M. Lázaro-Gredilla [b], D. Ramírez [c], J. Vía [a], I. Santamaría [a]

[a] Department of Communications Engineering, University of Cantabria, Spain
[b] Signal Theory and Communications, Universidad Carlos III de Madrid, Spain
[c] Signal and System Theory Group, University of Paderborn, Germany

ARTICLE INFO

*Article history:*
Received 23 November 2012
Received in revised form
24 September 2013
Accepted 2 October 2013
Available online 12 October 2013

*Keywords:*
Bayesian inference
Bayesian forgetting
Cognitive radio
Generalized likelihood ratio test (GLRT)
Multiantenna spectrum sensing

ABSTRACT

Recent work on multiantenna spectrum sensing in cognitive radio (CR) networks has been based on generalized likelihood ratio test (GLRT) detectors, which lack the ability to learn from past decisions and to adapt to the continuously changing environment. To overcome this limitation, in this paper we propose a Bayesian detector capable of learning in an efficient way the posterior distributions under both hypotheses. Our Bayesian model places priors directly on the spatial covariance matrices under both hypotheses, as well as on the probability of channel occupancy. Specifically, we use inverse-gamma and complex inverse-Wishart distributions as conjugate priors for the null and alternative hypotheses, respectively; and a binomial distribution as the prior for channel occupancy. At each sensing period, Bayesian inference is applied and the posterior for the channel occupancy is thresholded for detection. After a suitable approximation, the posteriors are employed as priors for the next sensing frame, which forms the basis of the proposed Bayesian learning procedure. The performance of the Bayesian detector is evaluated by simulations and by means of a CR testbed composed of universal radio peripheral (USRP) nodes. Both the simulations and experimental measurements show that the Bayesian detector outperforms the GLRT in a variety of scenarios.



**Contents**



☆ The research leading to these results has received funding from the Spanish Government (MIC INN) under Projects TEC2010-19545-C04-03 (COSIMA) and CONSOLIDER-INGENIO 2010 CSD2008-00010 (COMONSENS). It also has been supported by FPI Grant BES-2011-047647.

* Corresponding author. Tel.: +34 942200919 - 803.
*E-mail addresses:* juliocesar@gtas.dicom.unican.es (J. Manco-Vásquez), miguel@tsc.uc3m.es (M. Lázaro-Gredilla), david.ramirez@sst.upb.de (D. Ramírez), jvia@gtas.dicom.unican.es (J. Vía), nacho@gtas.dicom.unican.es (I. Santamaría).

0165-1684/$ - see front matter © 2013 Elsevier B.V. All rights reserved.
http://dx.doi.org/10.1016/j.sigpro.2013.10.005

## 1. Introduction

Cognitive radio (CR) networks [1–3] rely on spectrum sensing as a key operation that secondary users (SUs) must perform in order to identify whether a wireless communication channel is in use by a licensed primary user (PU) or not [4]. A reliable spectrum sensing stage is crucial to detect spectrum holes that can be subsequently filled with transmissions from SU [5]. To this end, detectors employing multiple antennas have received increased attention recently because they do not require prior knowledge about the PU signaling scheme and are able to work with asynchronously sampled signals [6–12]. These multiantenna detectors exploit the fact that under the null hypothesis (only noise) the signals received at the different antennas are spatially uncorrelated, whereas the presence of a PU induces some correlation and/or additional structure in the spatial covariance matrix.

Since the binary hypothesis testing problem involves some unknown parameters (e.g., noise variance and channel), the generalized likelihood ratio test (GLRT) approach has been typically followed to find one-shot detectors in several scenarios [6,7,9,12]. In [12], frequency and time-domain GLRTs have been derived that only exploit the spatial correlation induced by the presence of a PU, whereas the problem of detecting a rank-P primary user signal is addressed in [9,7]. However, these detectors do not take into account the smooth changes in the characteristics of the channel or the noise that can be expected between consecutive sensing frames. More precisely, it is reasonable to assume that the time scale of variation of the statistical parameters involved in the detection problem (for instance, noise variance or space–time PU activity pattern) are much longer than the sensing period. For instance, channel access patterns for primary users have been characterized as slowly time-varying in [13] and more recently in [14]. It is clear that detectors able to learn from past decisions would provide improved performance in these slowly time-varying scenarios. With this goal in mind, in this paper we propose an adaptive Bayesian framework for multiantenna sensing and evaluate its performance both by simulations and by means of a CR testbed.

Adaptive Bayesian detectors for radar applications have been proposed in [15–17], where a training set of data is available for the estimation of noise statistics. For cognitive radio applications, however, noise-only data is not always available; therefore, these adaptive Bayesian techniques cannot be applied to the scenarios considered in this paper. Bayesian detectors specific for cognitive radios have been previously proposed in [18–22]. Typically, these works assume a prior distribution for the unknown parameters and apply Bayesian inference to come up with improved parameter estimates and, consequently, more reliable detectors. In comparison to these Bayesian approaches, our work presents two main novelties: first, our Bayesian detector places priors directly on the spatial covariance matrices under both hypotheses; and second, it includes learning and forgetting steps that allow to track the variations of the channel and noise characteristics from frame to frame. Our Bayesian approach is able to learn from past sensing frames when the coherence time of the propagation channel [23] is longer than the time elapsed between consecutive sensing periods. We refer to this situation as “smooth channel variations”. Let us also remark that the proposed Bayesian detector is specifically tailored for multiantenna cognitive receivers and, consequently, this approach is not directly applicable to single-antenna SUs.

Specifically, our multiantenna Bayesian model uses inverse-gamma and complex inverse-Wishart distributions as conjugate priors for the null and alternative hypotheses, respectively; and a binomial distribution as the prior for channel occupancy. The reason for choosing these priors being that under Gaussian noise they are the conjugate priors for this problem and, therefore, the posteriors can be calculated in closed form. More precisely, the posterior conditioned on the channel state occupancy (idle or busy) adopts the same form as the prior. However, the unconditional posterior (marginalized over the channel state) becomes a convex combination of the priors. Since the marginalized or unconditional posteriors summarize the information gathered so far about the actual CR scenario, they are used as priors for the next sensing period: this represents the learning stage. To keep the learning process simple and scalable, the unconditional posterior (which is a linear combination of complex inverse-Wishart distributions when the PU is present) must be approximated within the family of the prior. Furthermore, the procedure is equipped with a forgetting mechanism based on [24] that allows to work on non-stationary environments.

In this paper, we extend some initial results about this Bayesian approach which were presented in [25,26]. In particular, we consider the optimal approximation of the unconditional posterior according to the Kullback–Leibler (KL) distance, and compare its performance and computational cost with the simple approximation based on thresholding, which was discussed in [25]. Also, we present a more in depth study of the proposed CR detector performance for different number of receiver antennas, observations and channel conditions. Finally, we also evaluate experimentally the performance of the proposed detector, in comparison to conventional GLRT-based detectors, using to this end a cognitive radio hardware platform based on Universal Software Radio Peripheral (USRP) devices [27].

The rest of the paper is organized as follows. The detection problem for the CR network is formulated in Section 2. The Bayesian inference procedure for a single sensing frame is presented in Section 3, where two different approximations of the posterior are derived. The learning and forgetting procedure for dealing with multiple sensing frames will be discussed in Section 4. In Section 5, we analyze the simulation results for different settings including both stationary and non-stationary environments, whereas the results obtained with the CR testbed are presented in Section 6. Finally, our main conclusions are summarized in Section 7.

## 2. Preliminaries

### 2.1. Notation

In this paper, we use bold-face lower case and bold-face upper case letters for column vectors and matrices, respectively; and light-face lower case letters for scalar quantities. The superscripts $\dot{(\cdot)}$ and $\tilde{(\cdot)}$ refer to the parameters of the posterior and prior distributions, respectively; and $\hat{(\cdot)}$ is used for estimated matrices and scalars. The determinant of a matrix $\mathbf{A}$ is denoted as $|\mathbf{A}|$, its trace as $\mathrm{tr}(\mathbf{A})$, the operator $\mathrm{diag}(\mathbf{A})$ refers to a diagonal matrix formed with the elements along the main diagonal of $\mathbf{A}$, $[\mathbf{A}]_{ij}$ denotes the $ij$ element of the matrix, and the superscript $(\cdot)^H$ denotes Hermitian transpose. Finally, $\mathbf{x}\sim\mathcal{CN}(\boldsymbol{\mu},\mathbf{R})$ indicates that $\mathbf{x}$ is a complex circular Gaussian random vector of mean μand covariance matrix $\mathbf{R}$.

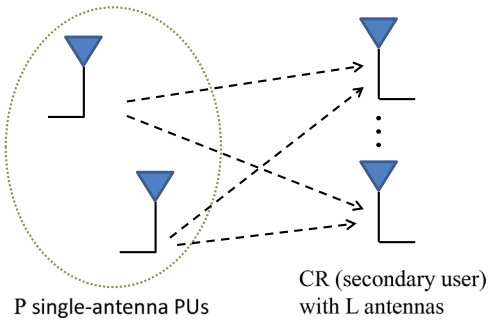


**Fig. 1.** CR detection model: a cognitive user with $L$ antennas tries to detect the presence of $P\geq 1$ single-antenna PUs or, equivalently, a single $P$-antenna PU.

### 2.2. Problem statement and GLRT detectors

We consider a cognitive receiver equipped with $L$ antennas that wants to detect whether the channel is occupied by a primary user or not. During the $t$-th sensing frame, the cognitive receiver acquires $n=0,\ldots,N-1$ snapshots denoted by $\mathbf{x}_t[n]\in\mathbb{C}^L$. The signal received during the $t$-th sensing period is stacked in a matrix: $\mathbf{X}_t=[\mathbf{x}_t[0],\ldots,\mathbf{x}_t[N-1]]$. The spectrum sensing problem can be formulated as a binary hypothesis test as follows:

$$\mathcal{H}_1:\mathbf{x}_t[n]=\mathbf{H}_t\mathbf{s}_t[n]+\mathbf{v}_t[n],$$
$$\mathcal{H}_0:\mathbf{x}_t[n]=\mathbf{v}_t[n], \tag{1}$$

where $\mathbf{x}_t[n]$ is the acquired snapshot at time $n$, $\mathbf{s}_t[n]\in\mathbb{C}^P$ is the primary signal vector, which might represent the signal emitted by a single PU with $P$ antennas or the signals emitted concurrently by $P$ single-antenna PUs (see Fig. 1), $\mathbf{H}_t\in\mathbb{C}^{L\times P}$ describes the multiple-input multiple-output (MIMO) channel between the PU and the cognitive receiver, and $\mathbf{v}_t[n]$ is modeled as zero-mean additive white Gaussian circular noise. In our model, both the channel $\mathbf{H}_t$ and the transmitted signal $\mathbf{s}_t[n]$ are assumed to be random quantities. More specifically, taking into account that any spatial correlation and scaling of the primary signal can be absorbed in the channel matrix, we model $\mathbf{s}_t$ as a zero-mean circular complex Gaussian, spatially white and power-normalized. Under these assumptions, the distributions of the vector-valued observations under each hypotheses $\mathcal{H}_1$ and $\mathcal{H}_0$ can be modeled as $\mathcal{CN}(\mathbf{0},\mathbf{R}_t)$ and $\mathcal{CN}(\mathbf{0},\mathbf{D}_t)$, respectively. Therefore, without any additional prior knowledge about the modulation format or signaling scheme used by the PU, the spectrum sensing problem amounts to testing between two different structures for the covariance matrix of $\mathbf{x}_t[n]$:

$$\mathcal{H}_1:\mathbf{x}_t[n]\sim\mathcal{CN}(\mathbf{0},\mathbf{R}_t),\quad n=0,\ldots,N-1,$$
$$\mathcal{H}_0:\mathbf{x}_t[n]\sim\mathcal{CN}(\mathbf{0},\mathbf{D}_t),\quad n=0,\ldots,N-1. \tag{2}$$

Under $\mathcal{H}_1$, the $L\times L$ covariance matrix $\mathbf{R}_t$ can be written as $\mathbf{H}\mathbf{H}^H+\mathbf{D}$, i.e., a rank-$P$ matrix plus a scaled diagonal matrix. In this paper, we assume that the rank $P$, the channel $\mathbf{H}$, and the noise variance are all unknown parameters; therefore, under the alternative hypothesis $\mathbf{R}_t$ has no further structure beyond being a positive semidefinite matrix. On the other hand, under $\mathcal{H}_0$, $\mathbf{D}_t$ is an arbitrary diagonal covariance matrix. In this way, our proposed Bayesian scheme is able to work in the most general setting.

Notice also that the likelihood under each hypothesis depends on unknown parameters and therefore the hypotheses are composite. The most typical approach to solve this kind of testing problems is the generalized likelihood ratio test (GLRT) [28]. When the noise is independent and identically distributed (iid) at each antenna ($\mathbf{D}_t=\sigma^2\mathbf{I}$) and $P\geq L-1$, the GLRT is the well-known

sphericity test [29],[1] which is given by

$$\mathcal{L}_S = \frac{|\mathbf{S}_t|^{1/L}}{(1/L)\mathrm{tr}(\mathbf{S}_t)} \tag{3}$$

where $\mathbf{S}_t = \mathbf{X}_t\mathbf{X}_t^H/N$ is the sample covariance matrix.

A more general testing problem that can accommodate calibration uncertainties in the different antenna front-ends takes into account a generic diagonal noise covariance matrix under $\mathcal{H}_0$. The GLRT in this case is the Hadamard ratio [30] and is given by

$$\mathcal{L}_H = \frac{|\mathbf{S}_t|}{\prod_{i=1}^{L}[\mathbf{S}_t]_{ii}}. \tag{4}$$

## 3. Bayesian inference on a single sensing frame

The Bayesian approach proposed in this paper assigns prior distributions to the covariance matrices under both hypotheses, as well as to the probability of channel occupancy. After discussing which priors should be used for this problem, in this section we perform exact Bayesian inference over a single sensing frame to derive the posteriors for the unknown parameters. Specifically, the posterior for the channel occupancy is the statistic used to decide whether the SU should transmit or not.

### 3.1. Prior distributions

Let us first introduce $z_t$ as a binary hidden random variable that indicates whether a transmitter is present ($z_t=1$) or not ($z_t=0$). Let us also remind that all our information about $\mathbf{R}_t$ and $\mathbf{D}_t$ is that they are some unknown covariance matrices, respectively full Hermitian and diagonal. Following a proper Bayesian treatment, prior distributions on all the unknown parameters of the model ($z_t$, $\mathbf{R}_t$ and $\mathbf{D}_t$) must be placed. We will use the following:

$$p(z_t) = \mathrm{Bernoulli}(z_t|\breve{\pi}_t) = \breve{\pi}_t^{z_t}(1-\breve{\pi}_t)^{1-z_t} \tag{5a}$$

$$p(\mathbf{R}_t) = \mathcal{CW}^{-1}\left(\mathbf{R}_t|\breve{n}_t,\breve{\mathbf{R}}_t\right) = \frac{|\breve{\mathbf{R}}_t|^{\breve{n}_t/2}|\mathbf{R}_t|^{-(\breve{n}_t+L+1)/2}\exp\left(-\frac{1}{2}\mathrm{tr}\left(\mathbf{R}_t^{-1}\breve{\mathbf{R}}_t\right)\right)}{2^{\breve{n}_tL/2}\Gamma_L\left(\frac{\breve{n}_t}{2}\right)} \tag{5b}$$

$$p(\mathbf{D}_t) = \mathcal{G}_L^{-1}\left(\mathbf{D}_t|\breve{m}_t,\breve{\mathbf{D}}_t\right) = \prod_{l=1}^{L}\mathcal{G}^{-1}\left([\mathbf{D}_t]_{ll}|\breve{m}_t/2,[\breve{\mathbf{D}}_t]_{ll}/2\right) = \frac{|\breve{\mathbf{D}}_t|^{\breve{m}_t/2}|\mathbf{D}_t|^{-(\breve{m}_t+L+1)/2}\exp\left(-\frac{1}{2}\mathrm{tr}\left(\mathbf{D}_t^{-1}\breve{\mathbf{D}}_t\right)\right)}{2^{\breve{m}_tL/2}\Gamma^L\left(\frac{\breve{m}_t}{2}\right)} \tag{5c}$$

where we have included the definitions of the Bernoulli distribution, the complex inverse-Wishart ($\mathcal{CW}^{-1}$) and the product of $L$ independent inverse-gamma ($\mathcal{G}_L^{-1}$). Note the difference between $\Gamma_L(\cdot)$ (used to denote the multivariate gamma function) and $\Gamma^L(\cdot)$ (the standard gamma function raised to the $L$-th power). We denote the parameters of the prior distributions as $\breve{\pi}_t, \breve{n}_t, \breve{\mathbf{R}}_t$, $\breve{m}_t$ and $\breve{\mathbf{D}}_t$. When the SU starts sensing the environment (i.e., at $t=0$), the priors should reflect our lack of knowledge about the sensed environment and, in this sense, they should be as uninformative as possible. In the Bayesian literature, typically Jeffreys uninformative priors [31] are used because they are invariant under reparametrizations (unlike a uniform prior). For our problem, and adopting a more practical point of view, starting with uninformative priors at $t=0$ amounts to choosing small initial parameters for the prior distributions (and 0.5 for the probability of channel occupancy). For instance, it can be proved that if $\breve{m}$ and $\breve{\mathbf{D}}$ tend to zero the product of $L$ independent inverse-gamma becomes Jeffreys' prior. Therefore, we simply chose small values for the prior parameters when the learning procedure starts. After that, the prior parameters are adapted and learnt over time as new sensing frames are acquired according to the mechanism that will be described in Section 4. For a more detailed discussion on the priors to be used for the multivariate Gaussian model the reader is referred to [32].

The main argument for the choice of these priors is analytical tractability: the complex inverse-Wishart distribution placed on $\mathbf{R}_t$ and the product of univariate inverse-gamma distributions placed on $\mathbf{D}_t$ are the conjugate priors for the distribution of full-rank covariance matrices and diagonal covariance matrices, respectively, when the observations follow a complex multivariate Gaussian distribution. As we will see in the next subsection, these conjugate priors allow us to exactly perform a Bayesian inference which is very convenient to avoid resorting to numerical integration methods. Nevertheless, let us also mention that several wireless standards use orthogonal frequency division multiplexing (OFDM) signals, which are typically modeled as zero-mean circular complex Gaussian signals, as well as MIMO technologies. For these practical scenarios, the signal model given in Eq. (1) and a flat prior for the covariance matrix reflecting our initial lack of knowledge about the main statistical parameters seem to be suitable.

### 3.2. Exact posterior distribution of $z_t$, $\mathbf{R}_t$ and $\mathbf{D}_t$

Since the noise is assumed to be Gaussian, the likelihoods of $p(\mathbf{X}_t|z_t=0,\mathbf{D}_t)$ and $p(\mathbf{X}_t|z_t=1,\mathbf{R}_t)$ can be written as

$$p(\mathbf{X}_t|z_t=0,\mathbf{D}_t) = \prod_{n=1}^{N}\mathcal{CN}(\mathbf{x}[n]|z_t=0,\mathbf{D}_t), \tag{6a}$$

$$p(\mathbf{X}_t|z_t=1,\mathbf{R}_t) = \prod_{n=1}^{N}\mathcal{CN}(\mathbf{x}[n]|z_t=1,\mathbf{R}_t). \tag{6b}$$

Given the hidden variable, $z_t$, priors are conjugate and therefore the posterior distributions (conditioned on the channel state) have the same form as the prior, but with different parameters. For instance, we have

$$p(\mathbf{R}_t|\mathbf{X}_t,z_t=1) = \mathcal{CW}^{-1}(\mathbf{R}_t|\hat{n}_t,\hat{\mathbf{R}}_t) \tag{7a}$$

$$p(\mathbf{D}_t|\mathbf{X}_t,z_t=0) = \mathcal{G}_L^{-1}(\mathbf{D}_t|\hat{m}_t,\hat{\mathbf{D}}_t). \tag{7b}$$

[1] For rank-deficient signal covariance matrices the GLRT is, in general, more complicated, as it was shown in [9].

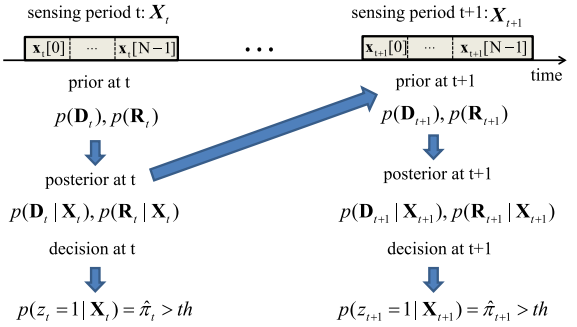


**Fig. 2.** A Bayesian framework for spectrum sensing: the posteriors obtained after processing a sensing frame are employed as priors for the next sensing frame.

where the posterior parameters, which clearly depend on the observed data $\mathbf{X}_t$, are given by

$$\hat{n}_t = \check{n}_t + N \tag{8a}$$

$$\hat{\mathbf{R}}_t = \check{\mathbf{R}}_t + \mathbf{S}_t \tag{8b}$$

$$\hat{m}_t = \check{m}_t + N \tag{8c}$$

$$\hat{\mathbf{D}}_t = \check{\mathbf{D}}_t + \mathrm{diag}(\mathbf{S}_t). \tag{8d}$$

When $z_t$ is marginalized (by a direct application of the total probability theorem), each unconditional posterior becomes a convex combination of the posteriors for each hypothesis, yielding

$$p(\mathbf{R}_t|\mathbf{X}_t) = \hat{\pi}_t \mathcal{CW}^{-1}(\mathbf{R}_t|\hat{n}_t, \hat{\mathbf{R}}_t) + (1-\hat{\pi}_t)\mathcal{CW}^{-1}(\mathbf{R}_t|\check{n}_t, \check{\mathbf{R}}_t) \tag{9a}$$

$$p(\mathbf{D}_t|\mathbf{X}_t) = \hat{\pi}_t \mathcal{G}_L^{-1}(\mathbf{D}_t|\check{m}_t, \check{\mathbf{D}}_t) + (1-\hat{\pi}_t)\mathcal{G}_L^{-1}(\mathbf{D}_t|\hat{m}_t, \hat{\mathbf{D}}_t), \tag{9b}$$

$$p(z_t|\mathbf{X}_t) = \mathrm{Bernoulli}(z_t|\hat{\pi}_t) \tag{9c}$$

where $\hat{\pi}_t$ is given by

$$\hat{\pi}_t = \frac{p(\mathbf{X}_t|z_t=1)p(z_t=1)}{p(\mathbf{X}_t|z_t=1)p(z_t=1) + p(\mathbf{X}_t|z_t=0)p(z_t=0)}. \tag{10}$$

Recall that in (9a) and (9b) we use a breve (˘) to denote the parameters of the *prior* distribution, whereas we use a hat (ˆ) to denote the parameters of the *posterior* distribution. Finally, the marginal likelihood $p(\mathbf{X}_t|z_t)$ can be obtained analytically as

$$\begin{aligned} p(\mathbf{X}_t|z_t=1) &= \int p(\mathbf{X}_t|z_t=1, \mathbf{R}_t)p(\mathbf{R}_t)\,\mathrm{d}\mathbf{R} \\ &= \frac{|\check{\mathbf{R}}_t|^{\check{n}_t/2}\Gamma_L\left(\frac{\hat{n}_t}{2}\right)}{\pi^{NL/2}|\hat{\mathbf{R}}_t|^{\hat{n}_t/2}\Gamma_L\left(\frac{\check{n}_t}{2}\right)} \end{aligned} \tag{11a}$$

$$\begin{aligned} p(\mathbf{X}_t|z_t=0) &= \int p(\mathbf{X}_t|z_t=0, \mathbf{D}_t)p(\mathbf{D}_t)\,\mathrm{d}\mathbf{D} \\ &= \frac{|\check{\mathbf{D}}_t|^{\check{m}_t/2}\Gamma\left(\frac{\hat{m}_t}{2}\right)^L}{\pi^{NL/2}|\hat{\mathbf{D}}_t|^{\hat{m}_t/2}\Gamma\left(\frac{\check{m}_t}{2}\right)^L}. \end{aligned} \tag{11b}$$

After the posterior has been computed, the probability of a transmitter being present given observations $\mathbf{X}_t$ is simply $p(z_t = 1|\mathbf{X}_t) = \hat{\pi}_t$. Thus, we can occupy the channel when the collision probability $\hat{\pi}_t$ is below some desired threshold.

## 4. Bayesian inference over multiple frames

### 4.1. Learning from past sensing frames

The (unconditional) posteriors after processing the $t$-th frame summarize all statistical information observed so far. Therefore, a natural learning mechanism is to use them as priors for the next sensing frame, as depicted in Fig. 2. More specifically, the proposed learning procedure is as follows: at each sensing frame the cognitive receiver updates the posterior distributions for $\mathbf{R}_t$ and $\mathbf{D}_t$ from priors existing at $t$ and the likelihood obtained from $\mathbf{X}_t$; then, these posteriors become the priors to be used at the sensing period $t+1$. The procedure is started with uninformative priors at $t=0$.

A problem with a direct application of this idea is that, after applying Bayesian inference, the posterior distributions for $\mathbf{R}_t$ and $\mathbf{D}_t$ are convex combinations of the posteriors under each hypotheses, see Eqs. (9a) and (9b); and therefore the posterior does not belong to the same family distribution of the prior. For instance, the prior for $\mathbf{R}_t$ is a complex inverse-Wishart and the posterior is a linear combination of two complex inverse-Wisharts. To keep the process simple and scalable, it would be convenient to find an approximation of the posteriors within the family of each respective prior. In the next subsections we describe two possible approximations that can be applied to this end.

#### 4.1.1. Thresholding-based approximation

A simple approximation to the posterior that falls within the same family as the prior can be obtained by truncating $\hat{\pi}_t$ to either 0 or 1, whichever it is closer. When this is done, Eqs. (9a) and (9b) directly yield a posterior in the same family as the prior. In that case, when $\mathcal{H}_1$ is more probable, the posterior is obtained by performing only updates (8a) and (8b), whereas in the opposite case, only updates (8c) and (8d) are needed.

#### 4.1.2. Kullback–Leibler approximation

A more rigorous approach is to find the approximation of the posteriors within the family of the priors that minimize the Kullback–Leibler distance. More precisely, the exact posteriors (reproduced here for convenience) are given by

$$\begin{aligned} p(\mathbf{R}_t|\mathbf{X}_t) &= \hat{\pi}_t \mathcal{CW}^{-1}(\mathbf{R}_t|\hat{n}_t, \hat{\mathbf{R}}_t) + (1-\hat{\pi}_t)\mathcal{CW}^{-1}(\mathbf{R}_t|\check{n}_t, \check{\mathbf{R}}_t), \\ p(\mathbf{D}_t|\mathbf{X}_t) &= \hat{\pi}_t \mathcal{G}_L^{-1}(\mathbf{D}_t|\check{m}_t, \check{\mathbf{D}}_t) + (1-\hat{\pi}_t)\mathcal{G}_L^{-1}(\mathbf{D}_t|\hat{m}_t, \hat{\mathbf{D}}_t). \end{aligned} \tag{12}$$

Our problem consists in finding the approximations of these posteriors

$$q(\mathbf{R}_t|\mathbf{X}_t) = \mathcal{CW}^{-1}(\mathbf{R}_t|\tilde{n}_t, \tilde{\mathbf{R}}_t), \tag{13a}$$

$$q(\mathbf{D}_t|\mathbf{X}_t) = \mathcal{G}_L^{-1}(\mathbf{D}_t|\tilde{m}_t, \tilde{\mathbf{D}}_t), \tag{13b}$$

that minimize the Kullback–Leibler (KL) divergence. Therefore, we have to solve the following optimization

problems:

$$\{\tilde{m}_t, \tilde{\mathbf{D}}_t\} = \underset{\tilde{m}_t, \tilde{\mathbf{D}}_t}{\operatorname{argmin}} \operatorname{KL}(p(\mathbf{D}_t|\mathbf{X}_t)||q(\mathbf{D}_t|\mathbf{X}_t)) \tag{14a}$$

$$\{\tilde{n}_t, \tilde{\mathbf{R}}_t\} = \underset{\tilde{n}_t, \tilde{\mathbf{R}}_t}{\operatorname{argmin}} \operatorname{KL}(p(\mathbf{R}_t|\mathbf{X}_t)||q(\mathbf{R}_t|\mathbf{X}_t)). \tag{14b}$$

Fortunately, each of these minimization problems can be solved analytically except for a line search. The details of the derivation are relegated to Appendix A, in the following we summarize the solution. In order to find $\{\tilde{m}_t, \tilde{\mathbf{D}}_t\}$ and $\{\tilde{n}_t, \tilde{\mathbf{R}}_t\}$, we first compute the following auxiliary quantities:

$$\mathbf{K}_D = \hat{\pi}_t \check{m}_t \check{\mathbf{D}}_t^{-1} + (1-\hat{\pi}_t)\hat{m}_t \hat{\mathbf{D}}_t^{-1} \tag{15a}$$

$$\mathbf{K}_R = \hat{\pi}_t \hat{n}_t \hat{\mathbf{R}}_t^{-1} + (1-\hat{\pi}_t)\check{n}_t \check{\mathbf{R}}_t^{-1} \tag{15b}$$

$$k_D = -\ln|\mathbf{K}_D| + \hat{\pi}_t \left( L\psi\left(\frac{\check{m}_t}{2}\right) - \ln|\check{\mathbf{D}}_t|\right) + (1-\hat{\pi})\left(L\psi\left(\frac{\hat{m}_t}{2}\right) - \ln|\hat{\mathbf{D}}_t|\right) \tag{15c}$$

$$k_R = -\ln|\mathbf{K}_R| + \hat{\pi}_t \left( \psi_L\left(\frac{\hat{n}_t}{2}\right) - \ln|\hat{\mathbf{R}}_t|\right) + (1-\hat{\pi})\left(\psi_L\left(\frac{\check{n}_t}{2}\right) - \ln|\check{\mathbf{R}}_t|\right) \tag{15d}$$

where $\psi(\cdot)$ is the digamma function, and $\psi_L(\cdot) = \sum_{l=1}^{L} \psi(\cdot + (1-l)/2)$ defines the multivariate digamma function.

We then have to solve the following non-linear equations using, for instance, a few iterations of the Newton–Raphson method:

$$k_D + L\ln(\tilde{m}_t) - L\psi\left(\frac{\tilde{m}_t}{2}\right) = 0, \tag{16a}$$

$$k_R + L\ln(\tilde{n}_t) - \psi_L\left(\frac{\tilde{n}_t}{2}\right) = 0. \tag{16b}$$

Finally, the covariance matrices $\tilde{\mathbf{D}}_t$ and $\tilde{\mathbf{R}}_t$ for the best approximation according to the KL distance are given by $\tilde{m}_t \mathbf{K}_{\mathbf{D}}^{-1}$ and $\tilde{n}_t \mathbf{K}_{\mathbf{R}}^{-1}$, respectively. These values are taken as the new parameters of the posterior distributions, that is

$$\tilde{\mathbf{D}}_t \to \hat{\mathbf{D}}_t, \tag{17a}$$

$$\tilde{\mathbf{R}}_t \to \hat{\mathbf{R}}_t, \tag{17b}$$

$$\tilde{n}_t \to \hat{n}_t, \tag{17c}$$

$$\tilde{n}_t \to \hat{m}_t. \tag{17d}$$

### 4.2. Forgetting in non-stationary environments

Since the channel may vary between consecutive frames, it is interesting to introduce a mechanism within the Bayesian framework to forget past data and hence be able to operate in a non-stationary environment. We assume here that no additional knowledge about the dynamical evolution of the channel, PU spectrum usage pattern or noise statistics is available. Therefore, we resort to the idea of Bayesian $\lambda$-forgetting [24] that allows us to forget in a principled manner with minimal assumptions. The basic idea of Bayesian forgetting is to use as prior distributions for frame $t+1$ a "smoothed" version of the posterior distributions obtained after processing frame $t$ and the original prior distributions for $\mathbf{R}_t$ and $\mathbf{D}_t$ given by (5), i.e.,

$$p(\mathbf{D}_{t+1}|\mathbf{X}_t) \propto p(\mathbf{D}_t|\mathbf{X}_t)^{\lambda} p(\mathbf{D}_0)^{1-\lambda}, \tag{18a}$$

$$p(\mathbf{R}_{t+1}|\mathbf{X}_t) \propto p(\mathbf{R}_t|\mathbf{X}_t)^{\lambda} p(\mathbf{R}_0)^{1-\lambda}. \tag{18b}$$

Observe that according to this definition, when $\lambda = 0$, all the information obtained from the previous data is forgotten and the process considers each frame independently (as the GLRT does), which is reasonable if abrupt changes occur in $\mathbf{R}_t$ and $\mathbf{D}_t$ between frames. When $\lambda = 1$, no forgetting occurs and the new posterior corresponds to the standard Bayesian posterior when $\mathbf{D}_t$ and $\mathbf{R}_t$ are constant across frames $\mathbf{D}_t = \mathbf{D}$, $\mathbf{R}_t = \mathbf{R}\ \forall t$, which is reasonable under stationary conditions. Values of $\lambda \in [0,1]$ are therefore appropriate to model different evolution speeds in the channel, without having to define a concrete dynamical model. In another perspective, Eqs. (18) represent a change of the posterior in the direction of the prior: this has also been named as "back-to-the-prior" forgetting in [33,34] and a method for the selection of the forgetting value can be found in [35].

With this forgetting step, the parameters of the prior distributions to be used for Bayesian inference at $t+1$ are given by

$$\check{n}_{t+1} = \lambda \hat{n}_t + (1-\lambda)\check{n}_0 \tag{19a}$$

$$\check{\mathbf{R}}_{t+1} = \lambda \hat{\mathbf{R}}_t + (1-\lambda)\check{\mathbf{R}}_0 \tag{19b}$$

$$\check{m}_{t+1} = \lambda \hat{m}_t + (1-\lambda)\check{m}_0 \tag{19c}$$

$$\check{\mathbf{D}}_{t+1} = \lambda \hat{\mathbf{D}}_t + (1-\lambda)\check{\mathbf{D}}_0. \tag{19d}$$

### 4.3. The proposed algorithm

The whole process is summarized in Algorithm 1. Since the algorithm only requires updating and storing $\hat{\mathbf{R}}_t$, $\hat{n}_t$, $\hat{\mathbf{D}}_t$, $\hat{m}_t$ from one frame to the next, it requires a fixed amount of memory and computation per sensing frame, which is $\mathcal{O}(L^2)$.

**Algorithm 1.** Online Bayesian multiantenna sensing.

1: Initialize Parameters: $\lambda$, $\check{\mathbf{R}}_0$, $\check{n}_0$, $\check{\mathbf{D}}_0$, $\check{m}_0$
2: **for** Frame $t = 1, 2, \ldots$ **do**
3: Sense the medium $N$ times through $L$ antennas to get $\mathbf{X}_t$
4: Exact posterior: Compute $\hat{\mathbf{R}}_t$, $\hat{n}_t$, $\hat{\mathbf{D}}_t$, $\hat{m}_t$ and $\hat{\pi}_t$ using (8) and (11)
5: Take a decision about the channel occupancy based on $\hat{\pi}_t$, which is the probability of a PU being present at $t$.
6: Compute the approximated posterior parameters using KL minimization or thresholding
7: Forget: Compute $\check{\mathbf{R}}_t$, $\check{n}_t$, $\check{\mathbf{D}}_t$, $\check{m}_t$ using Eqs. (19)
8: **end for**

Let us notice that our Bayesian detector minimizes the probability of error just by deciding that the channel is busy when $p(z_t = 1|\mathbf{X}_t)$ is greater than $p(z_t = 0|\mathbf{X}_t)$, or, in other words, when $p(z_t = 1|\mathbf{X}_t) > 0.5$. Notice also that, when the SU decides to transmit, the posterior probability for the channel occupancy can be translated into an "instantaneous" estimate of the false alarm probability. For instance, if $p(z_t = 1|\mathbf{X}_t) = 0.2$ and the SU decides to

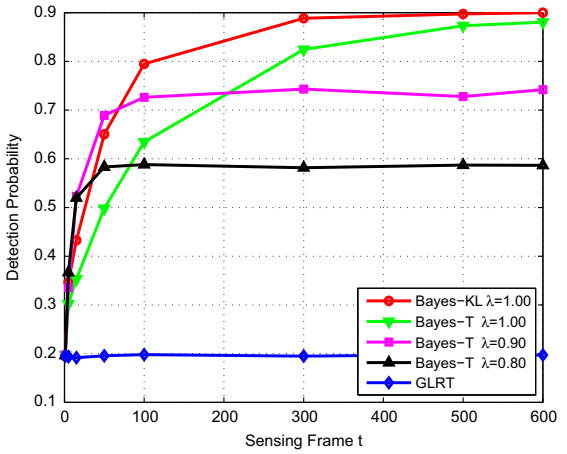


**Fig. 3.** $P_D$ for the Bayesian detector (Bayes-KL and Bayes-T) and the GLRT vs. the number of sensing frames in a time-invariant channel, $L=5$, $P=5$, $N=50$, SNR $=-8$ dB and $P_{FA}=0.1$.

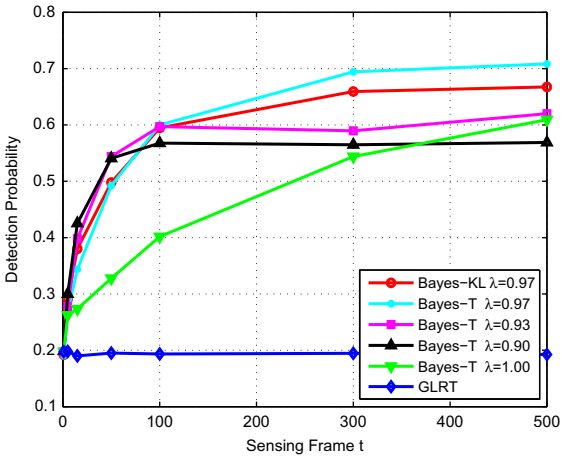


**Fig. 4.** $P_D$ for the Bayesian detector (Bayes-KL and Bayes-T) and the GLRT vs. the number of sensing frames in a slowly time-varying channel. $L=5$, $P=5$, $N=50$, SNR $=-8$ dB, $P_{FA}=0.1$ and $\lambda_{ch}=0.9$.

occupy the channel, the estimated probability of collision with the PU (i.e., a false alarm) would also be 0.2. Then, if we set the threshold $\eta=0.2$ we ensure that the instantaneous[2] $P_{FA}<0.2$. We consider this as an additional advantage of the proposed Bayesian procedure, for which we can easily identify the desired operation point (i.e, the threshold for the posterior probability of channel occupancy) just by assigning costs to the different decisions and setting the threshold accordingly.

Finally, we would like to stress that, for each new sensing frame, the proposed Bayesian scheme always updates the parameters of the posterior following the steps in Algorithm 1. Since we intend to operate in a probably changing environment, the sensing procedure must be continuously applied and we do not use any stopping rule.

## 5. Simulation results

In this section, we compare the performance of the proposed Bayesian detector with that of a GLRT-based detector (given by (4)) in different environments by means of Monte Carlo simulations. Unless otherwise stated, we assume a probability of channel occupancy given by $\breve{\pi}_t=0.5$, a primary transmitter with $P=5$ antennas and a secondary cognitive receiver with $L=5$ antennas. The MIMO channel matrix is assumed to be constant during the $t$-th sensing frame with i.i.d. entries distributed as $\mathcal{CN}(0,1)$. On the other hand, the channel evolves from frame to frame as $\mathbf{H}_{t+1}=\lambda_{ch}\mathbf{H}_t+(1-\lambda_{ch})\mathbf{P}_{t+1}$ [36], with $0\le\lambda_{ch}\le 1$, and $\mathbf{P}_{t+1}$ a complex Gaussian noise matrix also with i.i.d. entries distributed as $\mathcal{CN}(0,1)$. For $\lambda_{ch}=1$ we have a stationary channel, whereas for $\lambda_{ch}=0$ it changes independently from frame to frame as a block fading channel [37, Chapter 4, Section 4.2].

[2] This can be seen as a worst-case value, since $p(z_t=1|\mathbf{X}_t)=0.2$ does not necessarily mean that 20% of the times the PU is active in this scenario, it is just our estimate of the posterior probability.

### 5.1. $P_D$ vs. number of sensing frames

In this subsection, we study how the performance of the Bayesian detector evolves over time in stationary, slowly time-varying and fast time-varying environments. We start at $t=0$ with an uninformative prior (we use small values for the parameters of the prior distributions) and then after each sensing frame we update the posterior (learning step), approximate the posterior using either truncation (denoted as Bayes-T in the plots) or KL minimization (denoted as Bayes-KL) and finally forget moving the approximated posterior towards the original uninformative prior with a forgetting factor $\lambda$. As a figure of merit we plot the detection probability $P_D=P(\hat{\pi}_t>\eta|\mathcal{H}_1)$ vs. the number of sensing frames, where $\eta$ is the threshold. We consider a fixed false alarm probability of $P_{FA}=0.1$, and in each sensing frame the number of observations is $N=50$.[3] For comparison we include the results obtained with the GLRT. In all examples we use a signal-to-noise ratio SNR $=-8$ dB.

#### 5.1.1. Stationary channel

We first consider a static scenario for which the channel remains constant over all sensing frames (i.e., $\lambda_{ch}=1$). The results in Fig. 3 show that in this scenario, after just a few sensing frames, the Bayesian multiantenna detector provides a much higher $P_D$ than the GLRT for different values of the forgetting parameter $\lambda$. After

[3] The parameters in our simulations were not chosen to target any particular application or standard, since existing standards are mainly focused on static scenarios. In static scenarios, the sensing frames are typically much longer and the SNRs are also lower than those considered in our paper. As an example, the spectrum sensing requirements of the IEEE 802.22 wireless regional network (WRAN) standard establish that the miss detection should not exceed 0.1 subject to a $P_{FA}=0.1$ when the SNR $=-20.8$ dB, these requirements yield sensing periods of thousands of samples at a sampling rate of 21.52 MHz [38,39]. In our paper, we aimed at non-stationary environments and consequently considered much shorter (and frequent) sensing periods ($N=50$ samples) in which the block-fading model is assumed to be valid.

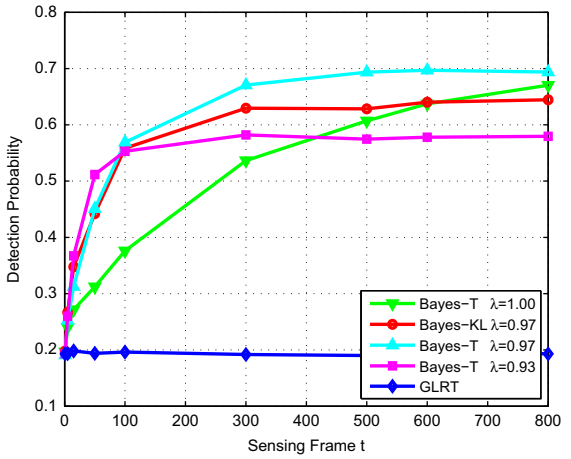


**Fig. 5.** $P_D$ for the Bayesian detector (Bayes-KL and Bayes-T) and the GLRT vs. the number of sensing frames in a fast time-varying channel. $L=5$, $P=5$, $N=50$, SNR $=-8$ dB, $P_{FA}=0.1$, and $\lambda_{ch}=0.1$.

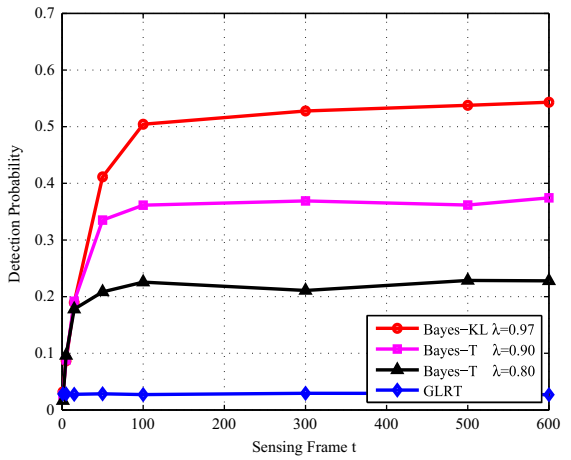


**Fig. 6.** $P_D$ for the Bayesian detector (Bayes-KL and Bayes-T) and the GLRT vs. the number of sensing frames in a time-invariant channel. $L=5$, $P=5$, $N=50$, SNR $=-8$ dB and $P_{FA}=0.01$.

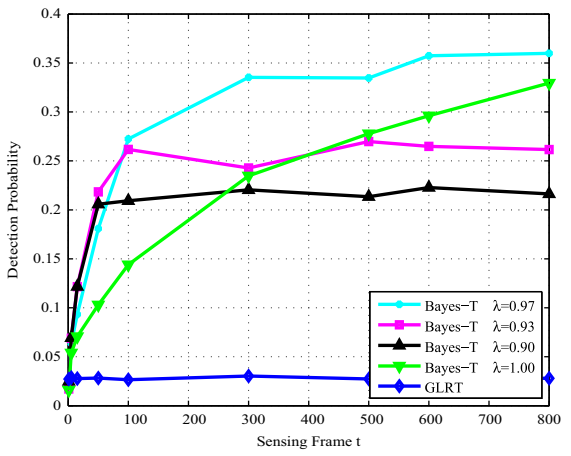


**Fig. 7.** $P_D$ for the Bayesian detector and the GLRT vs. the number of sensing frames in a slowly time-variant channel. $L=5$, $P=5$, $N=50$, SNR $=-8$ dB, $P_{FA}=0.01$ and $\lambda_{ch}=0.9$.

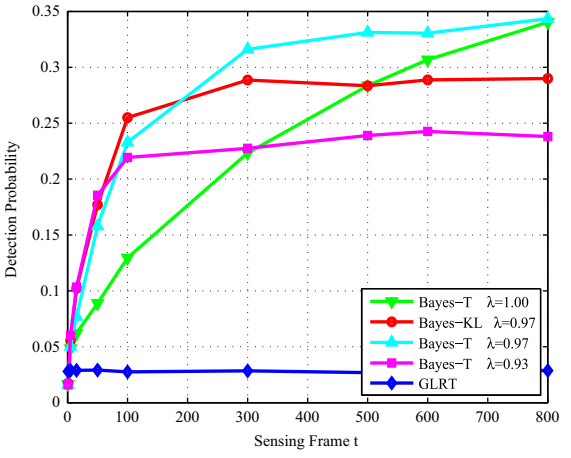


**Fig. 8.** $P_D$ for the Bayesian detector (Bayes-KL and Bayes-T) and the GLRT vs. the number of sensing frames in a fast time-variant channel. $L=5$, $P=5$, $N=50$, SNR $=-8$ dB, $P_{FA}=0.01$ and $\lambda_{ch}=0.1$.

observing a sufficient number of frames the best results are obtained when using $\lambda=1$ (which means no forgetting at all), as could be expected for this static environment. Interestingly, however, to forget a little ($\lambda=0.9$) can be beneficial during the first sensing frames. This is explained because during the first sensing frames detection errors are more likely to occur and, consequently, the parameters of the posterior are not updated correctly. In this situation, it would be better not to trust so much on the observed data and apply the forgetting step. Finally, we also compare in the figure the performance of the two approximations of the posterior proposed in the paper. As expected, the KL-based approximation provides a better performance at the cost of a higher computational complexity.

### 5.1.2. *Slowly time-varying channel*

We now consider a non-stationary environment created by a slowly time-varying channel with $\lambda_{ch}=0.9$. The results in Fig. 4 show again that the Bayesian detector outperforms the GLRT after just a few sensing frames. The optimal value of the forgetting factor, obtained by numerical results, for this scenario seems to be close to $\lambda=0.97$,[4] and using a value of $\lambda=1$ (no forgetting) strongly affects the performance. It is also clear that the convergence now is slower, since it takes more sensing frames to effectively learn and track the covariance matrices under both hypotheses. Finally, regarding the impact of the posterior approximation on the performance of the detector, we observe that in non-stationary environments it is better to use a thresholding-based approximation. In non-stationary environments, the importance of obtaining at each step an accurate approximation diminishes since the performance is limited by the variations observed from frame to frame.

### 5.1.3. *Fast time-varying channel*

In Fig. 5, we finally consider the case of a fast time-varying environment with $\lambda_{ch}=0.1$. Remarkably, even in this highly

[4] Let us point out that this value has no direct relationship with $\lambda_{ch}$, since $\lambda$ is a design parameter and $\lambda_{ch}$ is a characteristic of the channel.

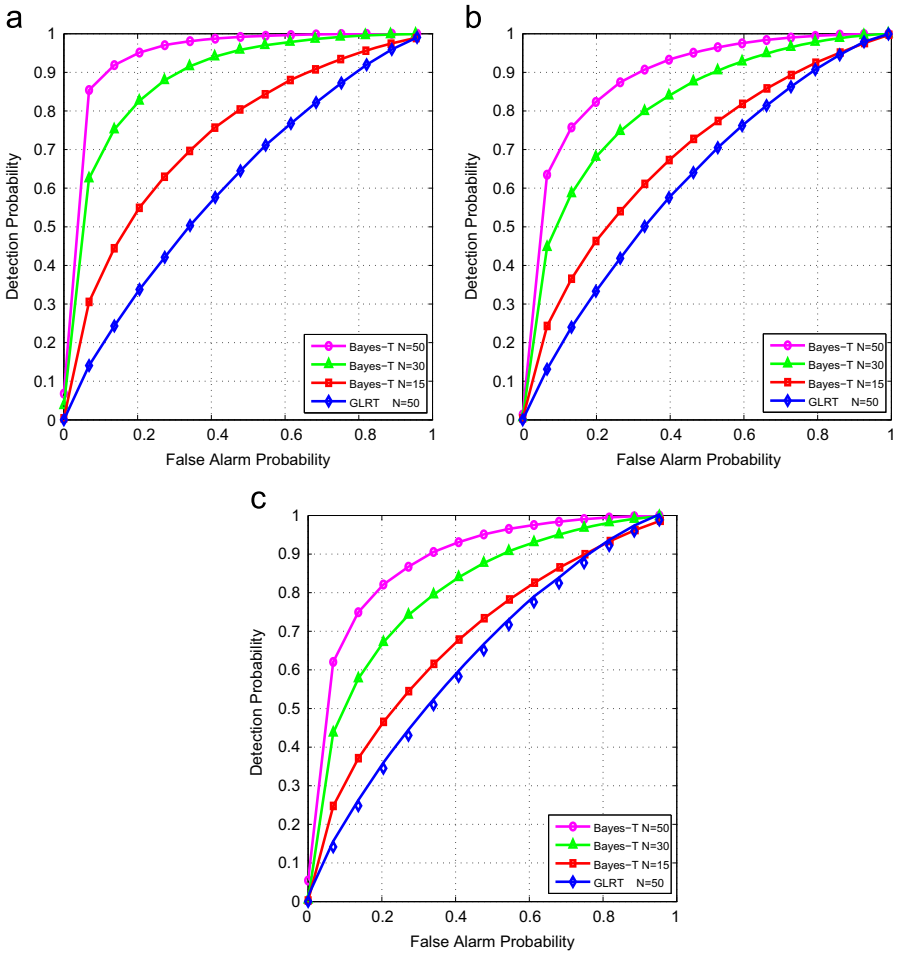


**Fig. 9.** ROC curves for the Bayesian and GLRT detectors with $L=5$, $P=5$ and different number of snapshots per sensing frame. (a) Stationary channel with SNR $=-8$ dB and $\lambda=1.0$. (b) Slowly time-varying channel with SNR $=-8$ dB, $\lambda=0.97$ and $\lambda_{ch}=0.90$. (c) Fast time-varying channel with SNR $=-8$ dB, $\lambda=0.97$ and $\lambda_{ch}=0.10$.

non-stationary environment, the Bayesian detector outperforms the GLRT detector. This improvement can be attributed to the fact that the covariance matrix under $\mathcal{H}_0$ remains almost constant from frame to frame (only the channel changes) and, therefore, it can be learnt by the Bayesian detector. This improved estimate of the noise-only covariance matrix translates into a better $P_D$ in comparison to the GLRT. For the reasons explained before, the simple truncation of the posterior performs better than the most accurate KL-based approximation in this rapidly varying scenario.

In order to provide a more complete understanding of the proposed method, we have repeated the experiments for $P_{FA}=0.01$. The new results for stationary, slowly time-varying and fast time-varying channels are depicted in Fig. 6, 7, and 8, respectively.

### 5.2. Receiver operating characteristic

In this subsection, we obtain the receiver operating characteristic (ROC) curve of the detector after convergence, i.e., after processing a sufficient number of frames to reach the steady state. We study the ROC curve for different number of observations per sensing frame ($N=\{50, 30, 15\}$). As we have seen previously, the approximation based on the KL distance is computationally more costly and does not provide any significant improvement in time-varying environments. Therefore, we concentrate on the results provided by the thresholding-based approximation referred to as Bayes-T, which seems to be better under non-stationary environments.

Fig. 9(a) shows the results for the stationary channel, with $\lambda=1$ and SNR $=-8$ dB. As we see, in steady-state the proposed Bayesian detector with only 15 snapshots per sensing frame outperforms the GLRT with 50 snapshots, which means a reduction of more than three times in the sensing time per frame. Fig. 9(b) and (c) shows the results for slowly (using $\lambda_{ch}=0.90$) and fast (using $\lambda_{ch}=0.10$) time-varying environments, respectively; from which similar conclusions can be drawn.

Finally, we fix the detection threshold and evaluate the probability of detection, $P_D$, and false alarm, $P_{FA}$, for different SNRs and in different scenarios. The number of

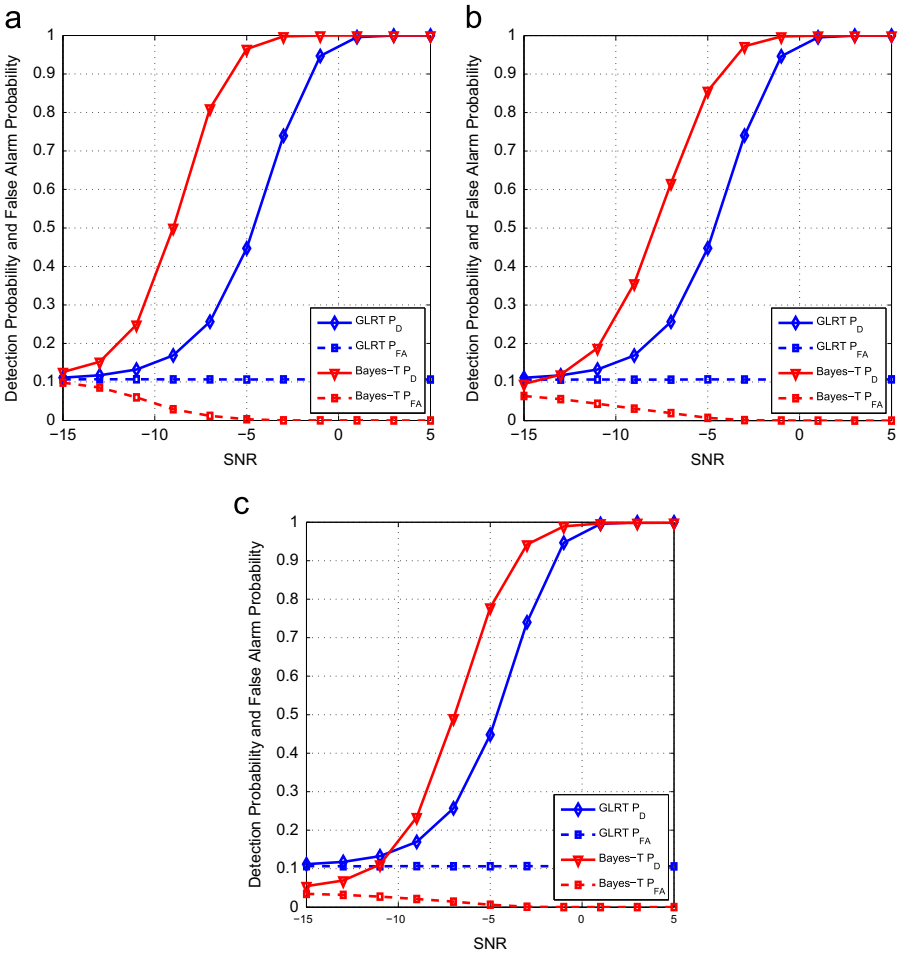


**Fig. 10.** $P_D$ and $P_{FA}$ vs SNR with $L=5$ antennas, and $N=50$. (a) In a time-invariant channel ($\lambda=1$ and $\lambda_{ch}=1$). (b) In a slowly time-varying channel ($\lambda=0.97$ and $\lambda_{ch}=0.95$). (c) In a fast time-varying channel ($\lambda=0.95$ and $\lambda_{ch}=0.10$).

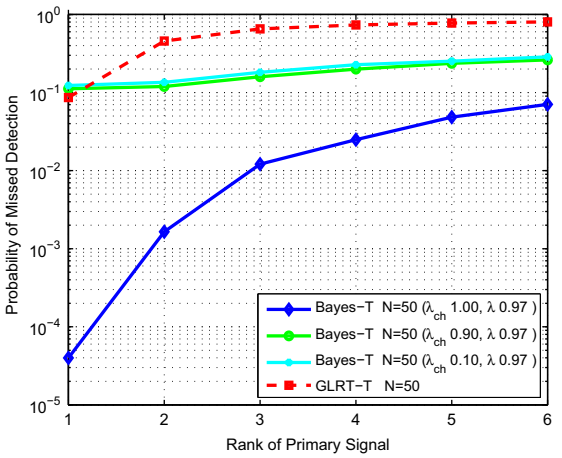


**Fig. 11.** Probability of missed detection vs. the rank of the primary signal $P$ for both detectors with $L=6$ antennas, $N=50$, SNR $=-8$ dB and $P_{FA}=0.1$. A static time-invariant channel with $\lambda=1.0$ using a KL posterior approximation, a slowly time-varying channel with $\lambda=0.97$ and $\lambda_{ch}=0.90$, and a fast time-varying channel with $\lambda=0.97$ and $\lambda_{ch}=0.10$.

samples per sensing frame is fixed to $N=50$ and the rest of parameters is the same as in the previous section. The results are shown in Fig. 10(a), (b) and (c) for stationary, slowly and fast time-varying scenarios, respectively.

### 5.3. Detection performance for a rank-P PU

In Fig. 11, we compare the probability of missed detection, $P_M$, for the Bayesian and GLRT detectors when the spatial rank of the PU signal varies. For the GLRT detector we have used the results in [9]. We consider a scenario with $L=6$, $N=50$, $P_{FA}=0.1$, $P=\{1,\ldots,6\}$ and SNR $=-8$ dB. In general, the performance of both detectors degrades for an increasing $P$, since as $P$ increases the covariance matrix under $\mathcal{H}_1$ has less structure to be exploited. Nevertheless, the Bayesian approach consistently provides better results than the GLRT, which validates again its ability to learn from the environment even when the actual model does not match exactly the presumed one.

**Fig. 12.** N210 Ettus devices with the XCVR2450 daughterboard installed. A two-antenna cognitive receiver is composed of two N210 boards connected through a MIMO cable.

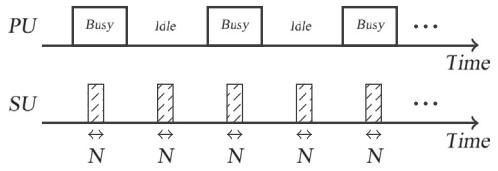


**Fig. 13.** A PU transmits according to a preestablished sequence of states, and the SU senses periodically the wireless channel.

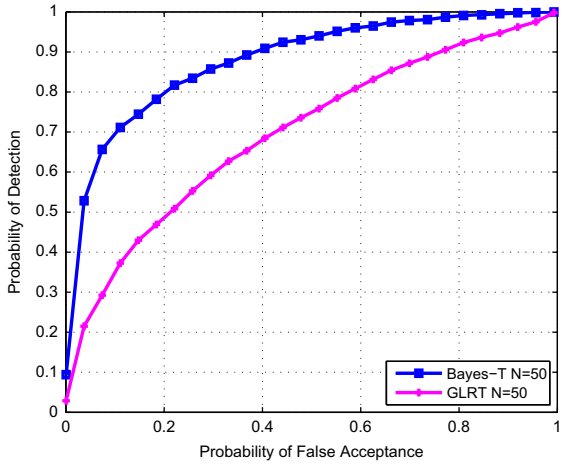


**Fig. 14.** ROC curves for the Bayesian and GLRT detectors using the CR platform in a realistic indoor channel at 5,6 GHz.

## 6. Experimental evaluation

In this section, we further validate the simulations by means of experimental measurements on a low-cost hardware cognitive platform. Specifically, our platform is composed of several N210 Universal Software Radio Peripheral (USRP) devices [27], each of them consists of a USRP motherboard and a Radio Frequency (RF) daughterboard (the XCVR2450 daughterboard based on a MAX2829 IC is able to cover ISM bands of 2.4–2.5 GHz, and 4.9–5.8 GHz). Basically, the motherboard consists of dual analog-to-digital converters (ADC) and digital-to-analog converters (DAC) connected to a Field Programmable Gain Array (FPGA). On the other hand, the daughterboard is a modular front-end used for analog operations such as up/down conversion.

In order to implement a multiantenna cognitive node, the N210 USRP includes a specific expansion port that allows coherent synchronization of two USRP2 units, as it is depicted in Fig. 12. Since the same clock (oscillators) and time reference are shared, both USRP nodes can start transmitting/receiving at the same time, thus avoiding any synchronization problem.

We have considered a simple scenario where a single-antenna PU accesses the channel according to a predefined pattern and a cognitive receiver with two antennas senses periodically the medium and applies different detection procedures. The platform is controlled from a central PC, which allows us to define a pattern of spectrum occupancy as well as the sensing periods (see Fig. 13). Therefore, at each sensing period we know exactly the true hypothesis and hence we can estimate $P_D$ and $P_{FA}$ for a given threshold.

The experiments were conducted in the laboratory of the Signal Processing Group at the University of Cantabria, with a clear line of sight (LOS) between the PU and the cognitive receiver in a rather static environment. The PU transmits an orthogonal frequency division multiplexing (OFDM) 802.11a signal with a rate of 9 Mbps using BPSK symbols at a carrier frequency of 5.6 GHz, although during the detection stage the modulation format is assumed to be unknown by the SU.

Previous works describing measurements carried out at 5 GHz band in the same scenario (see [40]) showed that the measured indoor channel presents long coherence times in comparison to time devoted to each experiment. Therefore, the measured scenario closely represents a stationary environment. For each experiment, the 2-antenna USRP node senses the spectrum over a period of several seconds and then a large amount of data is stored in an $L \times M$ matrix, where $M$ is the total number of samples and $L$ is the number of antennas. On the other hand, the activity of the PU, which is emulated by another USRP node, is controlled and recorded by a central PC. The activity pattern of the PU is recorded simultaneously while the SU is sensing the spectrum.

Using this data, the ROC curve is computed after processing 80 sensing frames so that our Bayesian detector reaches its steady-state performance. Since we know the channel status under which each sensing frame was acquired, the $P_{FA}$ and the $P_D$ can be easily estimated for different thresholds (to this end we used 5000 sensing frames) and the results depicted in Fig. 14 were obtained. The noise variance at each receiver antenna was measured and found to be very similar for the 2 RF branches, thus the Sphericity and Hadamard detectors [9] provided almost indistinguishable results which were both labeled in Fig. 14 as GLRT detector.

For each experiment, the SNR is controlled by the transmitter power and measured from the received signal at baseband. For the example shown here the measured SNR was $-7.3$ dB, the number of samples acquired by the

SU during each sensing frame was $N=50$, the number of SU antennas is $L=2$ and the number of PU antennas is $P=1$. In Fig. 14, we compare the ROC obtained by the proposed Bayesian detector working with a forgetting factor of $\lambda=0.99$ and the GLRT detector for this setup. This figure corroborates the validity of the simulations carried out in Section 5. For a full detailed description of the experimental evaluation, the reader is referred to [26,41], where a procedure to emulate time-varying scenarios is also described.

## 7. Conclusion

We have derived a new Bayesian framework for the problem of multiantenna spectrum sensing. We assume that the observations follow a Gaussian distribution under both hypotheses, which allow us to choose conjugate priors and thereby to perform the exact Bayesian inference with closed-form expressions. Moreover, our Bayesian framework is able to exploit previous statistical information obtained from past sensing frames. To that end, we propose a forgetting mechanism where the posterior densities on the covariance matrices summarize this past information and the next Bayesian inference takes these posteriors as suitable priors. We evaluate the derived Bayesian framework in different scenarios, that is, stationary and non-stationary environments. The comparison between the Bayesian framework and GLRT detector under these scenarios as well as experimental evaluations shows that the Bayesian detector outperforms the GLRT. The most interesting findings are provided under a time-varying environment, where we showed that the Bayesian detector is able to efficiently learn the posterior.

## Appendix A. Derivation of KL approximation

In this appendix we find the pdf approximation that is closest in terms of the KL distance to the exact posterior. For notational simplicity, we omit the subindex $t$ which refers to the sensing frame. We will only consider the approximation under $\mathcal{H}_1$, since the derivations under the null hypothesis are exactly the same. More precisely, under $\mathcal{H}_1$ the exact posterior is given by

$$p(\mathbf{R}|\mathbf{X})=\hat{\pi}\mathcal{CW}^{-1}(\mathbf{R}|\hat{n},\hat{\mathbf{R}})+(1-\hat{\pi})\mathcal{CW}^{-1}(\mathbf{R}|\check{n},\check{\mathbf{R}}), \tag{A.1}$$

and we want to find the approximation

$$q(\mathbf{R}|\mathbf{X})=\mathcal{CW}^{-1}(\mathbf{R}|\tilde{n},\tilde{\mathbf{R}}), \tag{A.2}$$

that minimizes the KL divergence. That is, we want to solve

$$\{\tilde{n},\tilde{\mathbf{R}}\}=\underset{\tilde{n},\tilde{\mathbf{R}}}{\operatorname{argmin}}\mathrm{KL}(p(\mathbf{R}|\mathbf{X})||q(\mathbf{R}|\mathbf{X})) \tag{A.3}$$

where

$$\mathrm{KL}(p(\mathbf{R}|\mathbf{X})\,\|\,q(\mathbf{R}|\mathbf{X}))=\int p(\mathbf{R}|\mathbf{X})\ln(p(\mathbf{R}|\mathbf{X}))\,\mathrm{d}\mathbf{R}-\int p(\mathbf{R}|\mathbf{X})\ln(q(\mathbf{R}|\mathbf{X}))\,\mathrm{d}\mathbf{R}. \tag{A.4}$$

The first term in the right hand side of (A.4) is the negative of the differential entropy of the exact posterior and hence does not depend on $\{\tilde{n},\tilde{\mathbf{R}}\}$. Therefore, minimizing the KL is equivalent to solving the following maximization problem:

$$\{\tilde{n},\tilde{\mathbf{R}}\}=\underset{\tilde{n},\tilde{\mathbf{R}}}{\operatorname{argmax}}\int p(\mathbf{R}|\mathbf{X})\ln(q(\mathbf{R}|\mathbf{X}))\,\mathrm{d}\mathbf{R}. \tag{A.5}$$

Now, by substituting (A.(1) and A.2) into (A.5), we have

$$\int p(\mathbf{R}|\mathbf{X})\ln(q(\mathbf{R}|\mathbf{X}))\,\mathrm{d}\mathbf{R}=\int\hat{\pi}\ln(\mathcal{CW}^{-1}(\mathbf{R}|\tilde{n},\tilde{\mathbf{R}}))\mathcal{CW}^{-1}(\mathbf{R}|\hat{n},\hat{\mathbf{R}})\,\mathrm{d}\mathbf{R}. +\int(1-\hat{\pi})\ln(\mathcal{CW}^{-1}(\mathbf{R}|\tilde{n},\tilde{\mathbf{R}}))\mathcal{CW}^{-1}(\mathbf{R}|\check{n},\check{\mathbf{R}})\,\mathrm{d}\mathbf{R}. \tag{A.6}$$

Integrating the first term on the right-hand side of Eq. (A.6) we get

$$\begin{aligned}
&\int\hat{\pi}\ln\left(\mathcal{CW}^{-1}\left(\mathbf{R}\middle|\tilde{n},\tilde{\mathbf{R}}\right)\right)\mathcal{CW}^{-1}\left(\mathbf{R}\middle|\hat{n},\hat{\mathbf{R}}\right)\mathrm{d}\mathbf{R}\\
&\quad=\hat{\pi}\left[\int\ln\left(\frac{|\tilde{\mathbf{R}}|^{\tilde{n}/2}}{2^{-\tilde{n}L/2}\Gamma_L\left(\frac{\tilde{n}}{2}\right)}\right)\mathcal{CW}^{-1}(\mathbf{R}|\hat{n},\hat{\mathbf{R}})\,\mathrm{d}\mathbf{R}\right]\\
&\qquad+\hat{\pi}\left[-\frac{\tilde{n}+L+1}{2}\int\ln|\mathbf{R}|\mathcal{CW}^{-1}\left(\mathbf{R}|\hat{n},\hat{\mathbf{R}}\right)\mathrm{d}\mathbf{R}\right]\\
&\qquad+\hat{\pi}\left[-\frac{1}{2}\int\mathrm{tr}\left(\mathbf{R}^{-1}\tilde{\mathbf{R}}\right)\mathcal{CW}^{-1}\left(\mathbf{R}\middle|\hat{n},\hat{\mathbf{R}}\right)\mathrm{d}\mathbf{R}\right]\\
&\quad=\hat{\pi}\left[\frac{\tilde{n}}{2}\ln|\tilde{\mathbf{R}}|-\frac{\tilde{n}}{2}L\ln(2)-\ln\Gamma_L\left(\frac{\tilde{n}}{2}\right)\right]\\
&\qquad+\hat{\pi}\left[-\frac{\tilde{n}+L+1}{2}\left(\ln|\hat{\mathbf{R}}|-L\ln(2)-\psi_L\left(\frac{\hat{n}}{2}\right)\right)\right]\\
&\qquad+\hat{\pi}\left[-\frac{1}{2}\mathrm{tr}\left(\hat{n}\hat{\mathbf{R}}^{-1}\tilde{\mathbf{R}}\right)\right]
\end{aligned}$$

where in the last step, we have used the fact that[5] $\mathbb{E}[\ln|\mathbf{R}|]=\ln|\hat{\mathbf{R}}|-L\ln(2)-\psi_L(\hat{n}/2)$ and $\mathbb{E}[\mathbf{R}^{-1}]=\hat{n}\hat{\mathbf{R}}^{-1}$. By the same procedure, the second term on the right-hand side of Eq. (A.6) is given by

$$\begin{aligned}
&\int(1-\hat{\pi})\ln\left(\mathcal{CW}^{-1}\left(\mathbf{R}|\tilde{n},\tilde{\mathbf{R}}\right)\right)\mathcal{CW}^{-1}\left(\mathbf{R}|\check{n},\check{\mathbf{R}}\right)\mathrm{d}\mathbf{R}\\
&\quad=(1-\hat{\pi})\left[\frac{\tilde{n}}{2}\ln|\tilde{\mathbf{R}}|-\frac{\tilde{n}}{2}L\ln 2-\ln\left(\Gamma_L\left(\frac{\tilde{n}}{2}\right)\right)\right]\\
&\qquad+(1-\hat{\pi})\left[-\frac{\tilde{n}+L+1}{2}\left(\ln|\check{\mathbf{R}}|-L\ln(2)-\psi_L\left(\frac{\tilde{n}}{2}\right)\right)\right]\\
&\qquad+(1-\hat{\pi})\left[-\frac{1}{2}\mathrm{tr}\left(\check{n}\check{\mathbf{R}}^{-1}\tilde{\mathbf{R}}\right)\right]
\end{aligned}$$

Combining the two terms yields $\int p(\mathbf{R}|\mathbf{X})\ln(q(\mathbf{R}|\mathbf{X}))\,\mathrm{d}\mathbf{R}$. In order to obtain the parameters that maximize this function, we have to take derivatives with respect to $\tilde{n}$ and $\tilde{\mathbf{R}}$ and equate them to zero. We first derive $\int p(\mathbf{R}|\mathbf{X})\ln(q(\mathbf{R}|\mathbf{X}))\,\mathrm{d}\mathbf{R}$ with respect to $\tilde{\mathbf{R}}$, that is

$$\hat{\pi}\left[\frac{\tilde{n}}{2}\tilde{\mathbf{R}}^{-1}-\frac{\hat{n}}{2}\hat{\mathbf{R}}^{-1}\right]+(1-\hat{\pi})\left[\frac{\tilde{n}}{2}\tilde{\mathbf{R}}^{-1}-\frac{\check{n}}{2}\check{\mathbf{R}}^{-1}\right]=0$$

where we have applied the identities $\partial\ln|\mathbf{\Sigma_1}|/\partial\mathbf{\Sigma_1}=(\mathbf{\Sigma_1}^T)^{-1}$ and $\partial\,\mathrm{tr}(\mathbf{\Sigma_2}\mathbf{\Sigma_1})/\partial\mathbf{\Sigma_1}=\mathbf{\Sigma_2}^T$. By defining $\mathbf{K}_R=\hat{\pi}\hat{n}\hat{\mathbf{R}}^{-1}+(1-\hat{\pi})\check{n}\check{\mathbf{R}}^{-1}$, it readily follows that $\tilde{\mathbf{R}}=\tilde{n}\mathbf{K}_R^{-1}$.

[5] Recall that $\psi_L(a)=(\partial/\partial a)\ln(\Gamma_L(a))=\sum_{l=1}^{L}\psi(a+(1-l)/2)$.

Now we take the derivative of $\int p(\mathbf{R}|\mathbf{X})\ln(q(\mathbf{R}|\mathbf{X}))\,d\mathbf{R}$ with respect to $\tilde{n}$, which is given by

$$\begin{aligned}\hat{\pi}\left[\frac{1}{2}\ln|\tilde{\mathbf{R}}|-\frac{L}{2}\ln(2)-\frac{1}{2}\psi_L\left(\frac{\tilde{n}}{2}\right)\right]\\ -\hat{\pi}\left[\frac{1}{2}\ln|\hat{\mathbf{R}}|\quad-\frac{L}{2}\ln(2)-\frac{1}{2}\psi_L\left(\frac{\hat{n}}{2}\right)\right]\\ +(1-\hat{\pi})\left[\frac{1}{2}\ln|\tilde{\mathbf{R}}|-\frac{L}{2}\ln(2)-\frac{1}{2}\psi_L\left(\frac{\tilde{n}}{2}\right)\right]\\ -(1-\hat{\pi})\left[\frac{1}{2}\ln|\check{\mathbf{R}}|-\frac{L}{2}\ln(2)-\frac{1}{2}\psi_L\left(\frac{\check{n}}{2}\right)\right]=0\end{aligned}$$

Finally using $\tilde{\mathbf{R}}=\tilde{n}\mathbf{K}_R^{-1}$, and defining $k_R=-\ln|\mathbf{K}_R|+\hat{\pi}(\psi_L(\hat{n}/2)-\ln|\hat{\mathbf{R}}|)+(1-\hat{\pi})(\psi_L(\check{n}/2)-\ln|\check{\mathbf{R}}|)$, the non-linear equation $k_R+L\ln\tilde{n}-\psi_L(\tilde{n}/2)=0$ is obtained. The same approach is followed to compute its counterpart under the hypothesis $\mathcal{H}_0$.

## References


[1] J. Mitola, G.Q. Maguire Jr., Cognitive radio: making software radios more personal, IEEE Personal Communications 6 (4) (1999) 13–18.

[2] S. Haykin, Cognitive radio: brain-empowered wireless communications, IEEE Journal on Selected Areas in Communications 23 (2) (2005) 201–220.

[3] I.F. Akyildiz, W.-Y. Lee, M.C. Vuran, S. Mohanty, Next generation dynamic spectrum access cognitive radio wireless networks: a survey, Computer Networks 50 (13) (2006) 2127–2159.

[4] T. Yucek, H. Arslan, A survey of spectrum sensing algorithms for cognitive radio applications, IEEE Communications Surveys & Tutorials 11 (1) (2009) 116–130.

[5] S.V. Nagaraj, Entropy-based spectrum sensing in cognitive radio, Signal Processing 89 (2) (2009) 174–180.

[6] P. Wang, J. Fang, N. Han, H. Li, Multiantenna-assisted spectrum sensing for cognitive radio, IEEE Transactions on Vehicular Technology 59 (4) (2010) 1791–1800.

[7] J. Sala-Alvarez, G. Vazquez-Vilar, R. Lopez-Valcarce, Multiantenna GLR detection of rank-one signals with known power spectrum in white noise with unknown spatial correlation, IEEE Transactions on Signal Processing 60 (6) (2012) 3065–3078.

[8] J. Tugnait, On multiple antenna spectrum sensing under noise variance uncertainty and flat fading, IEEE Transactions on Signal Processing 60 (4) (2012) 1823–1832.

[9] D. Ramirez, G. Vazquez-Vilar, R. Lopez-Valcarce, J. Via, I. Santamaria, Detection of rank-P signals in cognitive radio networks with uncalibrated multiple antennas, IEEE Transactions on Signal Processing 59 (8) (2011) 3764–3774.

[10] R. Zhang, T. Lim, Y.-C. Liang, Y. Zeng, Multi-antenna based spectrum sensing for cognitive radios: a GLRT approach, IEEE Transactions on Communications 58 (1) (2010) 84–88.

[11] A. Taherpour, M. Nasiri-Kenari, S. Gazor, Multiple antenna spectrum sensing in cognitive radios, IEEE Transactions on Wireless Communications 9 (2) (2010) 814–823.

[12] D. Ramirez, J. Via, I. Santamaria, L.L. Scharf, Detection of spatially correlated Gaussian times series, IEEE Transactions on Signal Processing 58 (10) (2010) 5006–5015.

[13] T. Clancy, B. Walker, Predictive dynamic spectrum access, in: Proceedings of the SDR Forum Technical Conference, 2006.

[14] M. Lopez, Spectrum Usage Models for the Analysis, Design and Simulation of Cognitive Radio Networks (Ph.D. Thesis), Universitat Politecnica de Catalunya, 2011.

[15] S. Bidon, O. Besson, J. Tourneret, A Bayesian approach to adaptive detection in nonhomogeneous environments, IEEE Transactions on Signal Processing 56 (1) (2008) 205–217.

[16] A.D. Maio, E. Conte, Adaptive detection in Gaussian interference with unknown covariance after reduction by invariance, IEEE Transactions on Signal Processing 58 (6) (2010) 2925–2934.

[17] K.J. Sohn, H. Li, B. Himed, Parametric GLRT for multichannel adaptive signal detection, IEEE Transactions on Signal Processing 55 (11) (2007) 5351–5360.

[18] J. Font-Segura, X. Wang, GLRT-based spectrum sensing for cognitive radio with prior information, IEEE Transactions on Communications 58 (7) (2010) 2137–2146.

[19] R. Couillet, M. Debbah, A Bayesian framework for collaborative multi-source signal sensing, IEEE Transactions on Signal Processing 58 (10) (2010) 5186–5195.

[20] E. Axel, E.G. Larsson, A Bayesian approach to spectrum sensing, denoising and anomaly detection, in: Proceedings of the IEEE International Conference on Acoustics, Speech and Signal Processing, 2009, pp. 2333–2336.

[21] R. Couillet, M. Debbah, Bayesian inference for multiple antenna cognitive receivers, in: Proceedings of the IEEE Wireless Communications and Networking Conference, WCNC 2009, vol. 6, 2009, pp. 1–6.

[22] Y. Jin, Cognitive multi-antenna radar detection using Bayesian inference, in: Proceedings of IEEE Sensor Array and Multichannel Signal Processing Workshop (SAM), 2012.

[23] F. Hlawatsch, G. Matz, Wireless Communications over Rapidly Time-Varying Channels, Elsevier Academic Press, 2011.

[24] R. Kulhavý, M.B. Zarrop, On general concept of forgetting, International Journal of Control 58 (4) (1993) 905–924.

[25] J. Manco-Vasquez, M. Lazaro-Gredilla, D. Ramirez, J. Via, I. Santamaria, Bayesian multiantenna sensing for cognitive radio, in: Proceedings of IEEE Sensor Array and Multichannel Signal Processing Workshop (SAM), 2012.

[26] J. Manco-Vasquez, J. Gutierrez-Teran, J. Perez-Arriaga, J. Ibañez, I. Santamaria, Experimental evaluation of multiantenna spectrum sensing detectors using a cognitive radio testbed, in: Proceedings of IEEE International Symposium on Signals Systems and Electronics (ISSSE), Potsdam, Germany, 2012.

[27] Ettus Research LLC. Universal Software Radio, URL ⟨http://www.ettus.com/, 2012.

[28] S. Kay, Fundamentals of Statistical Signal Processing: Detection Theory, Prentice Hall, Upper Saddle River, NJ, 1998.

[29] J.W. Mauchly, Significance test for sphericity of a normal n-variate distribution, Annals of Mathematical Statistics 11 (2) (1940) 204–209.

[30] S.S. Wilks, On the independence of k sets of normally distributed statistical variables, Annals of Mathematical Statistics 3 (3) (1935) 309–326.

[31] H. Jeffreys, An invariant form for the prior probability in estimation problems, Proceedings of the Royal Society of London, Series A, Mathematical and Physical Sciences 186 (2012) 453–461.

[32] D. Sun, J.O. Berger, Objective priors for the multivariate normal model, in: 8th World Meeting on Bayesian Statistics, Alicante, Spain, 2006, pp. 1–26.

[33] S. Van Vaerenbergh, M. Lazaro-Gredilla, I. Santamaria, Kernel recursive least-squares tracker for time-varying regression, IEEE Transactions on Neural Networks and Learning Systems 23 (8) (2012) 1313–1326.

[34] F. Perez-Cruz, S. Van Vaerenbergh, J. Murillo-Fuentes, M. Lazaro-Gredilla, I. Santamaria, Gaussian processes for nonlinear signal processing, IEEE Signal Processing Magazine 30 (4) (2013) 40–50.

[35] S.V. Vaerenbergh, I. Santamaria, M. Lazaro-Gredilla, Estimation of the forgetting factor in kernel recursive least squares, in: Proceedings of IEEE International Workshop on Machine Learning for Signal Processing (MLSP), 2012.

[36] K. Baddour, N. Beaulieu, Autoregressive modeling for fading channel simulation, IEEE Transactions on Wireless Communications 4 (4) (2005) 1650–1662.

[37] A. Goldsmith, Wireless Communications, Cambridge University Press, 2005.

[38] H.-S. Chen, W. Gao, D.G. Daut, Spectrum sensing using cyclostationary properties and application to IEEE 802.22 WRAN, in: Global Communications Conference, GLOBECOM, Washington, USA, 2007.

[39] C. Cordeiro, M. Ghosh, D. Cavalcanti, K. Challapali, Spectrum sensing for dynamic spectrum access of TV bands, in: 2nd International Conference on Cognitive Radio Oriented Wireless Networks and Communications, CrownCom, Orlando, USA, 2007.

[40] J. Gutiérrez, Ó. González, J. Pérez, D. Ramírez, L. Vielva, J. Ibáñez, I. Santamaría, Frequency-domain methodology for measuring MIMO channels using a generic test bed, IEEE Transactions on Instrumentation and Measurement 60 (3) (2011) 827–838.

[41] J. Gutiérrez, J. Ibañez, J. Perez, Beamforming-based emulation of spatial and temporal correlated MISO channels, in: Proceedings of IEEE International Symposium on Signals Systems and Electronics (ISSSE), Potsdam, Germany, 2012.